Developmental Biology 455 (2019) 19–31

Contents lists available at ScienceDirect

Developmental Biology

journal homepage: www.elsevier.com/locate/developmentalbiology

Original research article

The selector genes *midline* and *H15* control ventral leg pattern by both inhibiting Dpp signaling and specifying ventral fate

Pia C. Svendsen [1], Lindsay A. Phillips [1], Ashish R. Deshwar, Jae-Ryeon Ryu, Nima Najand, William J. Brook [*]

Alberta Children's Hospital Research Institute, Department of Biochemistry and Molecular Biology, Cumming School of Medicine, University of Calgary, 3330 Hospital Drive NW, Calgary, AB, T2N4N1, Canada

A B S T R A C T

mid and *H15* encode Tbx20 transcription factors that specify ventral pattern in the *Drosophila* leg. We find that there are at least two pathways for *mid* and *H15* specification of ventral fate. In the first pathway, *mid* and *H15* negatively regulate Dpp, the dorsal signal in leg development. *mid* and *H15* block the dorsalizing effects of Dpp signaling in the ventral leg. In loss- and gain-of-function experiments in imaginal discs, we show that *mid* and *H15* block the accumulation of phospho-Mad, the activated form of the Drosophila pSmad1/5 homolog. In a second pathway, we find *mid* and *H15* must also directly promote ventral fate because simultaneously blocking Dpp signaling in *mid H15* mutants does not rescue the ventral to dorsal transformation in most ventral leg structures. We show that *mid* and *H15* act as transcriptional repressors in ventral leg development. The two genes repress the Dpp target gene *Dad*, the laterally expressed gene *Upd*, and the *mid* VLE enhancer. This repression depends on the eh1 domain, a binding site for the Groucho co-repressor, and is likely direct because Mid localizes to target gene enhancers in PCR-ChIP assays. A *mid* allele mutant for the repressing domain (eh1), mid^{eh1}, was found to be compromised in gain-of-function assays and in rescue of *mid H15* loss-of-function. We propose that *mid* and *H15* specify ventral fate through inhibition of Dpp signaling and through coordinating the repression of genes in the ventral leg.

1. Introduction

A hallmark of animal development is that signals pattern cells within a tissue by inducing transcription factors to specify distinct fates and patterns. This occurs in large fields of cells, patterned by morphogens, and also in smaller clusters, where local cell-cell signaling specifies individual fates. A common theme is that the expression of a single transcription factor can often act as a genetic switch, driving cells to choose one fate rather than another. This process is nearly universal, acting to select progenitors from clusters of precursors, subdivide embryonic axes, regionalize tissue layers, or to segregate and subdivide secondary fields in limbs or organs. Thus, a central problem of developmental biology is to understand how one transcription factor, a 'selector gene', can coordinate radically different developmental outcomes (Curtiss et al., 2002; García-Bellido, 1975; Mann and Carroll, 2002). Selector genes are critical components of the genetic pathways controlling fly limb development. They encode transcription factors that promote region-specific fates in the eye-antenna, leg, or wing imaginal discs. Selector genes are both necessary to specify the fate of the region where they are expressed and sufficient to specify that fate when expressed ectopically in the opposite territory. Formally, selector genes act as genetic switches that choose between the two fates. Previously, we described the role of the redundant T-box genes *midline* (*mid*) and *H15*, which act as selector genes for ventral fate in the fly leg (Svendsen et al., 2009). Here we dissect the logic of how *mid H15* promote ventral fate in leg development.

The patterning of the dorsal/ventral (D/V) axis in the fly leg is controlled initially by the secreted morphogens Decapentaplegic (Dpp: a fly Bone morphogenetic protein, BMP) and Wingless (Wg: a fly Wnt) (Fig. 1A). Dpp is expressed at high levels in the dorsal region and at a lower level in the ventral region of the leg imaginal disc but the ventral expression plays no apparent role in D/V patterning (Held and Heup, 1996). Dpp is necessary and sufficient to specify dorsal fate; Wg, expressed in the ventral region of the disc, is necessary and sufficient to specify ventral fate (Brook and Cohen, 1996; Heslip et al., 1997; Jiang and Struhl, 1996; Johnston and Schubiger, 1996; Morimura et al., 1996; Penton and Hoffmann, 1996; Theisen et al., 1996). The action of Dpp or Wg is not restricted solely to dorsal or ventral cells as the two signals act in concert to specify distal fate (Estella and Mann, 2008; Estella et al., 2008; Lecuit and Cohen, 1997). Ventral cells are exposed to both signals and the acquisition of ventral versus dorsal fate is controlled by the expression of *mid H15*. We showed that *mid H15* are activated in ventral cells by Wg and restricted from dorsal cells by Dpp and genes

* Corresponding author.
E-mail address: brook@ucalgary.ca (W.J. Brook).
[1] Equal contributions.

https://doi.org/10.1016/j.ydbio.2019.05.012
Received 9 September 2018; Received in revised form 27 April 2019; Accepted 28 May 2019
Available online 9 July 2019
0012-1606/

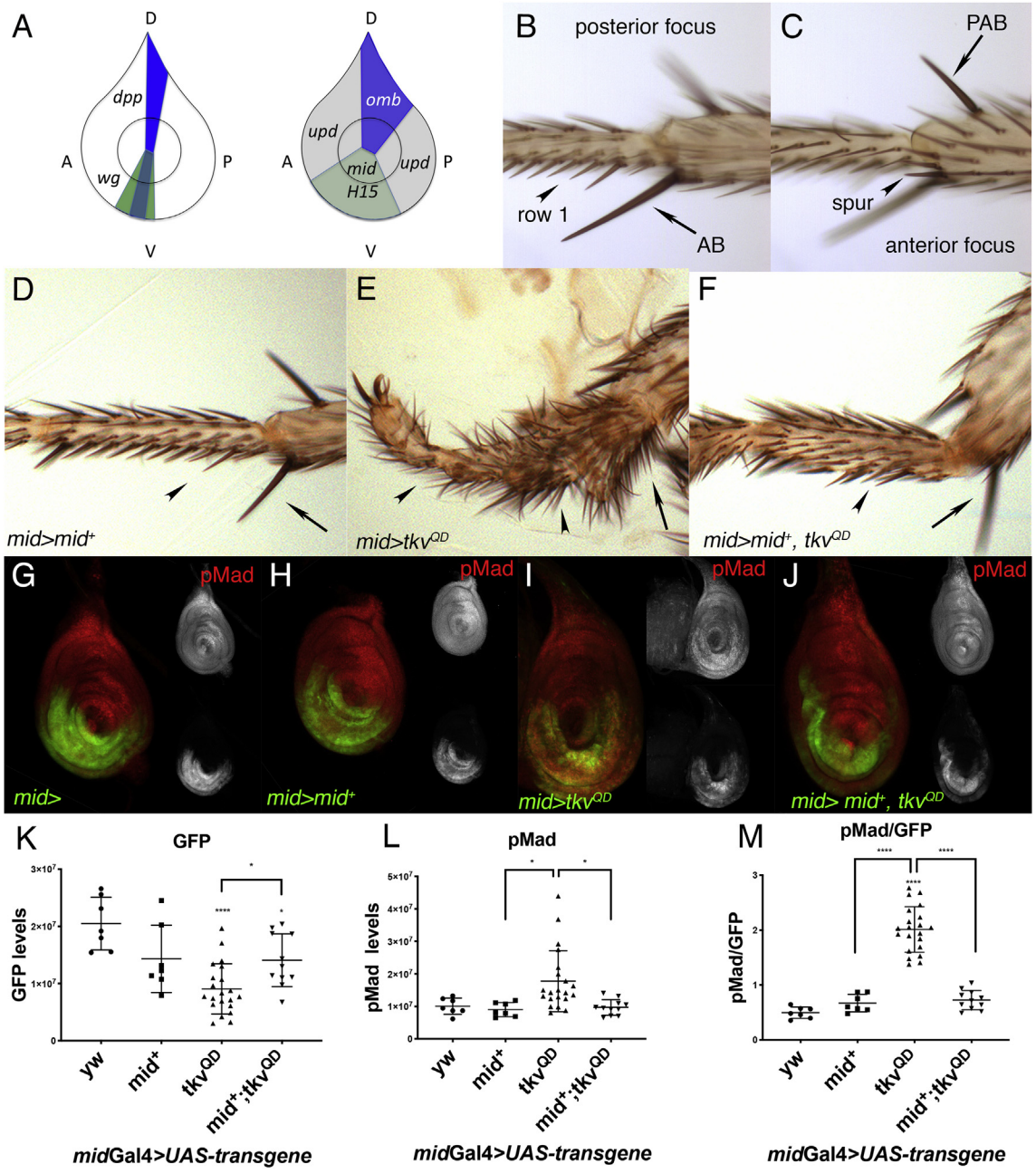

Fig. 1. Mid antagonizes Dpp signaling. (A) Cartoons depicting expression domains of *dpp* (blue, dorsal and weaker ventral expression) and *wg* (green, ventral), and target genes *H15* and *mid* (green, ventral), *omb* (blue, dorsal) and *Upd* (grey, lateral) in leg imaginal discs. Throughout the figures, leg imaginal discs are presented with dorsal up. Adult legs are oriented distal left and dorsal up. (B, C) Distal, wild type second leg showing proximal basitarsus and distal tibia. (B) Posterior focal plane showing the apical bristle (AB, on tibia, arrow) and row 1/8 pegs (on basitarsus, arrowhead). (C) Anterior focal plane showing the dorsal preapical bristle (PAB, arrow) and ventral spurs (C, arrowhead). The AB is longer and more distal than the PAB. (D–F) Cuticle from second legs with *mid*-Gal4 driving expression of UAS-*mid*-V5 *(mid^+)* (D), UAS-tkv^{QD} (E), or (F) UAS-*mid*-V5 *(mid^+);* UAS-tkv^{QD}. AB (arrow) and row 1/8 (arrowhead) have ventral character (D). Ventral expression of UAS-tkv^{QD} causes ventral bristles to be transformed to dorsal (E, row 1/8 peg to rapier, arrowheads, absence of AB, arrow). With co-expression of UAS-mid^+ and UAS-tkv^{QD}, AB is rescued (arrow) as are some pegs (arrowhead). Panels (G–J) show pMad staining (red and upper inset) and GFP expression (green and lower inset) in leg imaginal discs of (G) *mid*Gal4>UAS-*GFP* control, (H) *mid*Gal4>UAS-mid^+; UAS-*GFP* (I) *mid*Gal4>UAS-tkv^{QD}; UAS-*GFP*, (J) *mid*Gal4>UAS-mid^+; UAS-tkv^{QD}; UAS-*GFP*. Increased ventral levels of pMad induced by UAS-tkv^{QD} (I) are rescued by co-expression of UAS-mid^+ (J). Graphs (K–M) showing GFP levels (K), pMad levels (L) and pMad levels normalized to GFP levels (M) for discs represented in (G–J). Statistics used are Tukey's multiple comparisons test, with bars representing standard deviation, significance is indicated, * (P value 0.01 to 0.05) and **** (P value < 0.0001).

downstream of Dpp (Brook and Cohen, 1996; Svendsen et al., 2015). *mid* and *H15* act redundantly to specify all ventral fate. In the absence of *mid H15,* ventral structures are either transformed to dorsal fate or lost (Svendsen et al., 2009). These fate transformations resemble *wg* loss-of-function; indeed, all *wg*-dependent ventral structures (Held et al., 1994) are transformed in *mid H15* mutant clones. However, transformation due to *wg* loss-of-function is accompanied by increased expression of the dorsal determinant Dpp, which organizes ectopic dorsal pattern surrounding the clone (Brook and Cohen, 1996; Heslip et al., 1997; Jiang and Struhl, 1996; Theisen et al., 1996). In contrast, *mid H15* mutant clones are autonomously transformed to dorsal and neither express *dpp* nor cause non-autonomous patterning defects (Svendsen et al.,

2009). This indicates that *mid H15* are necessary to suppress dorsal fate but not to repress the expression of the dorsal gene *dpp*. However, *mid* and *H15* can each specify ventral fate when expressed ectopically. Thus, *mid H15* can be considered selector genes for ventral fate based on this necessity and sufficiency (Svendsen et al., 2009).

Here we test how *mid H15* execute selector function in D/V leg development. While *mid H15* are essential for the formation of ventral fate downstream of Wg, there are many possibilities for how they could function in the D/V pathway to specify ventral instead of dorsal. *mid H15* could act to repress a default dorsal fate, acting only to prevent the specification of dorsal fate through the action of the Dpp pathway and Dpp target genes. Some combination of both these and other pathways are also possible. In this study, we use genetic epistasis with the Dpp pathway to test the default fate in D/V development with respect to *mid H15* and *dpp*. We then analyze mid^{eh1}, a mutation in the engrailed-homology (eh1) domain that is compromised for repressing functions of Mid (Formaz-Preston et al., 2012) and find that the eh1 domain is essential for regulation of *mid H15* target genes and for the specification of ventral fate by *mid*. We find that there are different requirements for *mid* in different ventral structures, suggesting that *mid* specifies ventral fate through more than one genetic pathway.

2. Materials and methods

2.1. Fly stocks and transformant constructs

Flies were grown under standard conditions on cornmeal/glucose/yeast food at 25C. Stocks were obtained from Bloomington Indiana Stock Center (NIH P40OD018537) or were described previously (Buescher et al., 2004; Svendsen et al., 2009, 2015). The triple mutant $Mad^{1.2}$ (Wiersdorff et al., 1996) and $H15^{X4}$ mid^{1a5} was generated by recombination. The UAS-Flag-mid^{wt8a}, UAS-Flag-mid^{wt9b}, and UAS-mid^{eh1} (F41E) mid constructs (Formaz-Preston et al., 2012), and the UAS-$mid^{2.8}$ lines were previously generated. UAS-*mid*-V5 was constructed similarly to *Flag-mid*, adding a V5 tag to full length *mid* coding sequence and cloned into pUAST. Flies were co-transformed with helper plasmid Δ2-3 generating random insertion sites. Note that UAS-mid^{+} may refer to any of UAS-Flag-mid^{wt8a}, UAS-Flag-mid^{wt9b}, UAS-$mid^{2.8}$, or UAS-*mid*-V5. Different UAS-mid^{+} lines were selected for use based on chromosome linkage. Please refer to figure legends for the genotype used in each experiment.

2.2. Ectopic expression, genetic mosaics and MARCM analysis

Ectopic expression was performed using Gal4/UAS at 25C (Svendsen et al., 2009). Gain-of-function clones were generated by heat shock induction of hs-FLP at 48–72hr after egg laying (ael) to generate Gal4 expressing clones with P{*Ay*Gal4}25 (*Act* > *y*+>Gal4) (Ito et al., 1997). Cuticle clones were marked by the absence $yellow^{+}$. Clones in discs were labelled by UAS-*GFP* expression. Mosaic loss-of-function clones were generated using the FLP/FRT technique (Xu and Rubin, 1993) at 48–72 or 72–96h after egg laying (ael). The MARCM technique (Lee and Luo, 1999), using the line *UAS-GFP hsFLP* y^{1} w^{*}*; [y+ 25F Tub80]#8 FRT40A*; *Tub*Gal4/*TM6*, together with a *mid H15* FRT40A stock carrying UAS--Flag-mid^{wt8a} (mid^{+}) or UAS-mid^{eh1} mutant transgene was used to generate clones at 48–72 and 72–96hr ael and test for rescue in cuticle clones. Leg cuticle was prepared as in (Svendsen et al., 2009).

2.3. Reporter constructs, immunohistochemistry and imaging

The expression of the *Dad, Upd, omb, and H15* genes was detected using the *Dad*-lacZ (Tsuneizumi et al., 1997), *Upd*-lacZ (Sun et al., 1995), *omb*-lacZ (Grimm and Pflugfelder, 1996) and *H15*-lacZ (Brook et al., 1993) enhancer-traps, respectively. *mid* expression was visualized using the *VLE*-lacZ construct (Svendsen et al., 2015). Imaginal discs were labelled (Pattatucci and Kaufman, 1991) and visualized using confocal microscopy. Mouse-anti-β-galactosidase (1:1000, Promega) and rabbit-anti-β-galactosidase were used to detect expression from lacZ reporters. Rabbit-anti-NMR1 (1:2000) which recognizes H15 was kindly provided by Sandra Leal, University of Southern Mississippi, (Leal et al., 2009), rat-anti-Gsb-n (line 9A-1) was provided by Bob Holmgren (Northwestern University) and mouse-anti-Lbe was provided by Krzysztof Jagla (Clemont-Ferrand). Mouse-anti-Wingless (1:50; 4D4) and mouse anti-Scr (1:100, 6H4.1c) were obtained from Developmental Studies Hybridoma Bank (DSHB, created by the NICHD of the NIH and maintained at The University of Iowa, Department of Biology, Iowa City, IA 52242). We visualized pMad using a cross-reacting antibody to pSmad1/5/9 (from rabbit, 1:200, Cell Signaling Technology) and an antibody to Mad (from rabbit, 1:100, a gift from Laurel Raftery, University of Nevada, Las Vegas). Secondary antibodies were Alexa-fluor 546 and 488 to rabbit or mouse (1:500; Molecular Probes, Inc.; see also Key Resources Table). To quantify fluorescence intensity, Z-projections of discs were generated using ImageJ software (National Institutes of Health) and measurements were made in ImageJ following a previously published method (McCloy et al., 2014). Statistical analysis was performed with GraphPad Prism 7 (GraphPad Software) using either two-tailed unpaired *t*-test for single comparisons or ANOVA with Tukey's test for multiple comparisons.

2.4. Western blotting

Western blotting was performed similar to what is described in Wodarz (2008). 100 stage 10–12 (4h20 to 9h20 ael) embryos (genotypes noted in Supplemental Fig. 3 legend) were homogenized in 30 μl of SDS-loading buffer. 15 μl of the lysate was run on a 12% SDS polyacrylamide gel. The gel was transferred onto an activated PVDF membrane. Ponceau stained membrane was cut in half directly above the 55 kDa ladder band. Standard methods were used to probe the top half of the membrane with a 1:1000 dilution of mouse anti-flag antibody to detect tagged Mid protein (Sigma F1804) and the bottom half with a 1:10000 dilution of mouse anti-β-tubulin as a loading control (DSHB E7-C). HRP conjugated sheep anti-mouse (GE Healthcare NA931) was the detecting secondary antibody. Membranes were developed using ECL Prime Western Blotting Detection Reagent (GE Healthcare RPN2232) and Hyperfilm ECL (GE Healthcare 28906839). Developed film was scanned using a flatbed scanner and quantitated using Adobe Photoshop.

2.5. Chromatin immunoprecipitation

Chromatin immunoprecipitation (ChIP) was performed on isolated *mid*Gal4>UAS-Flag-mid^{wt9b}, *UAS*-Flag-mid^{wt8a} leg imaginal discs using a protocol modified from (Estella and Mann, 2008). For each of three biological samples produced, sheared chromatin from approximately 50 leg imaginal disc equivalents were used in each immunoprecipitation. The chromatin immunoprecipitation for the experimental sample was performed with mouse-anti-M2Flag antibody (Sigma); the chromatin was subsequently isolated and purified from a mixture of Protein A/G beads (Invitrogen) in 50 μl. Unpublished ChIP-seq results on triplicate biological samples were used to identify Flag-Mid peaks and select genes for PCR-ChIP validation and potential target gene analysis. Standard PCR reactions were performed on 2–5 μl samples of immunoprecipitated chromatin using the following primers: *Dad13*: *Dad*13For 5′-GTCAA ACCGGCTGACAAACC-3′, *Dad*13Rev 5′-GAGCGAGAGGGAAATGCC TG-3' (amplifying *D. melanogaster* genomic region chr3R:17056281–17056448; Release 6); *Upd3*: *Upd3*For 5′-TTGTCGAGGGGCGTTACC-3′, *Upd*3Rev 5′- ACGGCGGTTTTCATCTTTGC-3' (amplifying genomic region chrX:18273600–18273877); *VLE*: *VLE*For 5′-GGTATGGTTTTGGCAA TTGGC-3′, *VLE*Rev 5′- CTTCGGCAAAGGAACAGTCG-3' (amplifying genomic region chr2L:5501782–5501957).

Supplementary information is available in the Key Resources table.

2.6. Key resources table

REAGENT or RESOURCE	SOURCE	IDENTIFIER
Antibodies		
Mouse monoclonal anti-Scr (clone 6H4.1; D. Brower)	Developmental Studies Hybridoma Bank (DSHB)	Cat#anti-Scr 6H4.1; RRID: AB_528499
Mouse monoclonal anti-wg (clone 4D4; S. M. Cohen)	Developmental Studies Hybridoma Bank (DSHB)	Catanti-wg 4D4 RRID: AB_528512
Mouse monoclonal anti-B-Tubulin (clone E7; M. Klymkowsky)	Developmental Studies Hybridoma Bank (DSHB)	Cat#anti-Btubulin; RRID: AB_2315513
Rabbit anti-β-galactosidase	Jackson ImmunoResearch Laboratories, Cedarlane	
Mouse monoclonal anti-β-galactosidase	Promega	Cat#Z3781; RRID: AB_430877
mouse anti-M2FLAG	Sigma	Cat#F1804; RRID: AB_262044
Rabbit anti-P-Smad1/5/9	Cell Signaling Technology	Cat#(S463/465)/(S465/467)D5B10) 13820S
Rabbit anti-Mad	Laurel Raftery, University of Nevada, Las Vegas, NV, USA.	
Rabbit anti-NMR1	Jim Skeath, Washington University School of Medicine, St. Louis, MO, USA	Leal et al. (2009)
Rat-anti-Gsb-n monoclonal antibody (Lines 9A1)	Dr. Bob Holmgren, Northwestern University, Evanston, IL USA	Zhang et al. (1994)
Mouse-anti-Lbe monoclonal antibody	Dr. Kristoph Jagla, Clermont-Ferrand	Jagla et al. (1997)
Alexa Fluor 546 Goat anti-rabbit	Molecular Probes Inc.	A11035, Lot 584959
Alexa Fluor 488 Goat anti-rabbit	Molecular Probes Inc.	A11094, Lot 47207A
Alexa Fluor 546 Goat anti-mouse	Molecular Probes Inc.	A11030, Lot 517979
Alexa Fluor 488 Goat anti-mouse	Molecular Probes Inc.	A11029, Lot 564513
Alexa Fluor 546 Goat-anti-rat	Molecular Probes Inc.	A11081, Lot 58080A
ECL Anti-mouse IgG, Horseradish Peroxidase Linked Whole Antibody (sheep)	Amersham, GE Healthcare	NA931
Chemicals, Peptides, and Recombinant Proteins		
Formaldehyde (methanol free),10% UltraPure EM grade	Polysciences (Sigma)	Cat#04018-1
Complete mini EDTA-free, Protease Inhibitor Cocktail tablets	Roche (Sigma)	Cat#11836170001
Experimental Models: Organisms/Strains		
D. melanogaster: y[1] w[*]; Mad[1.2]	Lecuit et al. (1996)	
D. melanogaster: y[1] w[*]; H15[X4] mid[1a5]	Svendsen et al. (2009)	
D. melanogaster: y[1] w[*]; Mad[1.2]	Wiersdorff et al. (1996)	
D. melanogaster: y[1] w[*]; Mad[1.2] H15[X4] mid[1a5]/CyO	This paper	
D. melanogaster: H15-lacZ *b cn*	Brook et al. (1993)	
D. melanogaster: Dad-lacZ	Tsuneizumi et al. (1997)	
D. melanogaster: midVLE-lacZ	Svendsen et al. (2015)	
D. melanogaster: omb-lacZ	Grimm and Pflugfelder (1996)	
D. melanogaster: Upd-lacZ	Sun et al. (1995)	
D. melanogaster: UAS-*mid*Flag*[wt9b];* UAS-*mid*Flag*[wt8a]*	Formaz-Preston et al. (2012)	
D. melanogaster: UAS-*mid*Flag*[eh1]*	Formaz-Preston et al. (2012)	
D. melanogaster: UAS-*mid*-V5	This paper	
D. melanogaster: UAS-*GFPS65T[T2]*	BDSC	BDSC#1521
D. melanogaster: UAS-*GFPS65T[T10}*	BDSC	BDSC#1522
D. melanogaster: UAS-*tkv[QD]*	Lecuit et al. (1996)	
D. melanogaster: UAS-*arm[s10]*	Pai et al. (1997)	
D. melanogaster: UAS-*Lef[dn]*	Riese et al. (1997)	
*D. melanogaster: y[1] w[1]; Ay*Gal4*[25]* UAS-*GFP[T2]*	BDSC	BDSC#4411
D. melanogaster: y[1] w[1118];; Ubi-GFP[33] neoFRT]40A	BDSC	BDSC#5189
D. melanogaster: y[1] w[1118]; y+[25F] neoFRT[40A]	BDSC	BDSC#1816
D. melanogaster: omb-Gal4	Lecuit et al. (1996)	
D. melanogaster: dpp-Gal4	Staehling-Hampton et al., 1994	
D. melanogaster: da-Gal4	BDSC	BDSC
D. melanogaster: NP2113-Gal4 *(mid*-Gal4*)/CyO*	Hatashi et al., 2002	
D. melanogaster: P{w[+mC]=UAS-*mCD8::GFP.L}Ptp4E [LL4], P{ry[+t7.2]=hsFLP}22, y[1] w[*]; y+25F Tub*-Gal80 *FRT40A; tub*-Gal4*/TM6*	This paper from BDSC lines	MARCM rescue
y[1]w[1]; H15[X4] mid[1a5]; UAS-*mid[wt8a]*	This paper	MARCM rescue
y[1]w[1]; H15[X4] mid[1a5]; UAS-*mid[eh1]*	This paper	MARCM rescue
Oligonucleotides		
Primers for VLE PCR-ChIP	This paper	
For 5′-GGTATGGTTTTGGCAATTGGC-3′		
Rev 5′- CTTCGGCAAAGGAACAGTCG-3′		
Primers for Dad PCR-ChIP	This paper	
For 5′-GTCAAACCGGCTGACAAACC-3′		
Rev 5′-GAGCGAGAGGGAAATGCCTG-3′		
Primers for Upd PCR-ChIP	This paper	
For 5′-TTGTCGAGGGGCGTTACC-3′		
Rev 5′- ACGGCGGTTTTCATCTTTGC-3′		

3. Results

3.1. Mid antagonizes Dpp signaling

Many bristles have distinct cell fates along the dorsal ventral axis of the fly leg (Fig. 1B and C). Here we focus on the distal tibia and basitarsus of the second leg, which are particularly rich in dorsal and ventral-specific structures. Easily scored second leg structures include the ventral apical bristle (AB) (Fig. 1B), which is opposite and distal to the dorsal pre-apical bristle (PAB) (Fig. 1 C), and the ventral row 1/8 bristles (Fig. 1B and C), which are peg-shaped, and are opposite the dorsal row 4/5 bristles which are rapier-shaped. The ventral spur bristles (Fig. 1C) have no dorsal counterpart, neither do the first leg ventral-specific structures the sex comb bristles and transverse row bristles. We showed previously that *mid H15* specify ventral fate. For the ventral-specific AB and row 1/8 bristles (peg-shaped), the loss of *mid* and *H15* results in transformation to the dorsal PAB and row 4/5 bristles (rapier-shaped) respectively. Loss of *mid H15* causes spur bristles to transform to a structure that may be either lateral or dorsal in fate and the sex comb and transverse bristles in the first leg are simply missing. Ectopic *mid* (or *H15,* unpublished) expression in the dorsal region of the imaginal disc induces ectopic AB, spurs, row 1/8 and sex comb bristles, especially in dorsal lateral regions (Svendsen et al., 2009). In principle, *mid H15* could be instructive for ventral fate, overriding a default dorsal program. Another possibility is that they simply inhibit dorsal fate to allow the expression of a default ventral fate. Loss of *mid H15* function in ventral clones does not lead to increased expression of *dpp* or to induction of the dorsal T-box gene *omb* (Svendsen et al., 2009). This means that the ventral to dorsal transformation is not due to transcriptional de-repression of *dpp* or *omb* in the absence of *mid.* However, Dpp in the ventral leg does activate the Dpp pathway as seen by the presence of phosphorylated Mothers-against-decapentaplegic protein (pMad) in ventral cells (Azpiazu and Morata, 2002; Manjon et al., 2007). Mad is an rSmad, a transcription factor that mediates the effects of Dpp-signaling upon phosphorylation by the Dpp receptors, therefore pMad is an indicator of active Dpp signaling (Newfeld et al., 1997). Thus, the function of *mid* in the ventral leg could be to inhibit the effects of Dpp signaling.

In order to test whether *mid* function blocks the effects of Dpp signaling in the ventral leg, we examined the effects of expressing *mid* and an activated form of the Dpp receptor *thick veins (tkv^{QD})* (Lecuit et al., 1996) in the ventral leg under UAS control. *mid* and *H15* are redundant and UAS-*mid*$^{+}$ is sufficient to rescue *mid H15* loss-of-function, thus we use UAS-*mid*$^{+}$ alone in over-expression. We tested whether clones expressing UAS-*mid*$^{+}$ in the dorsal domain caused a cell-autonomous decrease in the levels of pMad labelling. Increased expression of UAS-*mid*$^{+}$ in the *mid* domain had little effect on leg development (n = 47) (Fig. 1D). In contrast, expression of UAS-*tkv*^{QD} in the *mid* domain caused a transformation of ventral structures into dorsal. In a sample of 44 legs, phenotypes included a transformation of ventral row 1/8 bristles to more dorsal fates and transformation of the ventral AB into a PAB bristle along with an overall shortening and malformation of the leg (Fig. 1E). Consistent with a role of Mid in antagonizing Dpp, the effects of UAS-*tkv*^{QD} expression were suppressed by co-expressing UAS-*mid*$^{+}$ (Fig. 1F). In a sample of 54 legs, none were as extreme as what was observed when expressing UAS-*tkv*^{QD} alone. We saw ventral to dorsal transformation in the ventral leg in clones of cells expressing UAS-*tkv*^{QD} under Act5C control (Fig S1A). Co-expression of UAS-*mid*$^{+}$ in clones partially suppresses these effects (Fig S1B). We also controlled for the number of UAS-transgenes in the different strains and found that UAS transgene copy number does not account for the decreased suppression of the ventral phenotypes (Fig S1C-F).

3.2. Mid and H15 block Dpp signaling downstream of receptor activation

To our surprise, the effects of UAS-*mid*$^{+}$ on the UAS-*tkv*^{QD} leg phenotype were correlated with changes in the levels of pMad observed in the different genotypes. We measured the levels of pMad within the GFP expression domain in *mid*Gal4 leg imaginal discs expressing UAS-*GFP* and UAS-*mid*$^{+}$ and/or UAS-*tkv*^{QD}. We controlled for levels of transgene expression by measuring the expression of UAS-*GFP* and then comparing the ratio of pMad to GFP in wild type and the three UAS genotypes. The levels of pMad in *mid*Gal4>UAS-*mid*$^{+}$ discs were similar to control discs (Fig. 1G, H, L) whereas the levels of GFP (Fig. 1K) were slightly reduced in these discs compared to controls due to the negative autoregulation of *mid* which decreases the level of Gal4 expression (Svendsen et al., 2015). As expected, the levels of pMad were much higher in *mid*Gal4>UAS-*tkv*^{QD} discs and the GFP levels were further reduced (Fig. 1I). The reduction in GFP was expected because Dpp signaling is a repressor of *mid* expression and should decrease the activity of *mid*Gal4 (Svendsen et al., 2015). However, the levels of pMad were not elevated when UAS-*mid*$^{+}$ was co-expressed with UAS-*tkv*^{QD} (Fig. 1J). There is lower overall activation of the Dpp pathway as indicated by pMad levels in *mid*Gal4>UAS-*mid*$^{+}$; UAS-*tkv*^{QD} discs (Fig. 1J,L). This decrease occurs despite higher levels of Gal4 driven transgene expression associated with this genotype as indicated by the relative GFP levels (Fig. 1M). In addition to using the levels of GFP as an internal control for expression, we also controlled for the number of UAS-transgenes and found that UAS transgene copy number does not account for the decreased pMad accumulation in genotypes expressing both UAS-*mid*$^{+}$ and UAS-*tkv*^{QD} (Fig S1G-J).

These results suggest that *mid H15* function antagonizes Dpp signaling. Consistent with *mid H15* function blocking Dpp signaling, the high levels of ventral *mid H15* expression and the higher levels of pMad staining form a boundary in the distal leg (Fig. 2A). To test this model, we asked whether UAS-*mid*$^{+}$ expression affected the levels of pMad. We first examined the effects of loss-of-function for *mid H15* on pMad. We induced clones lacking *mid H1*5 by mitotic recombination during larval development and marked by the absence of GFP. In 19 out of 27 clones in the ventral pSmad domain, we found cell-autonomous increases of pMad labelling either throughout the clone (Fig. 2B) or that expanded near the margins of the clone (Fig. 2C) when the clone overlapped the edge of the pMad domain. We also tested the effects of ectopic UAS-*mid*$^{+}$ expression on pMad accumulation. However, like the effects on pMad labelling in *mid H15* loss-of-function, these assays were hampered by the variable detection by the antibody (not shown). To circumvent this, we expressed UAS-*tkv*^{QD} under the control of the *Act5c*Gal4. This results in high levels of pMad in clones (Fig. 2D). When UAS-*mid*$^{+}$ is co-expressed in the clones, the levels of pMad are greatly reduced (Fig. 2E). The levels of GFP in both types of clone are comparable. Controlling for the number of UAS-transgenes in clones shows the reduction is due to the presence of mid and not due to titration of the Gal4 (Fig S2A,B). Finally, using an antibody that recognizes all forms of Mad, cells expressing UAS-*tkv*^{QD} have very high levels of Mad nuclear localization compared to non-expressing neighboring cells (Fig. 2F). In contrast, the distribution of Mad in cells expressing both UAS-*mid*$^{+}$ and UAS-*tkv*^{QD} is very similar to non-expressing neighboring cells (Fig. 2G). Thus, *mid* is necessary and sufficient to block the accumulation of pMad downstream of receptor activation. Taken together these results suggest that Mid not only blocks the effects of Dpp but that it does so by reducing Dpp signaling itself. Clearly, one of the roles for *mid H15* function in ventral fate specification is to override the effects of Dpp activation in the ventral leg.

3.3. Blocking Dpp signaling rescues some but not all ventral fate in mid H15 mutant tissue

Is inhibition of Dpp signaling the only function for *mid H15* in ventral leg development? In order to get a more precise picture of how *mid H15* interact with Dpp signaling in the ventral leg, we generated *mid H15* null clones that were unable to transduce the Dpp signal because they were also mutant for a strong hypomorphic allele of *Mad (Mad$^{1.2}$)* (Wiersdorff et al., 1996). If Mid acts to suppress dorsal fate downstream of Dpp, clones mutant for *mid H15*, which are normally transformed to dorsal fate

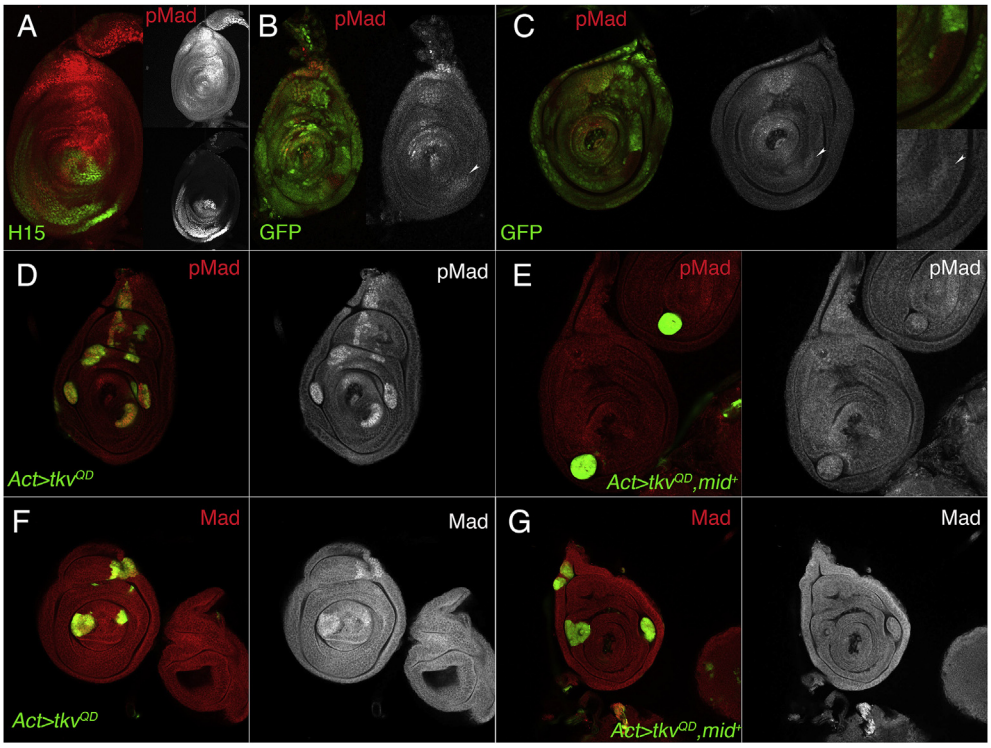

Fig. 2. Mid inhibits Dpp signaling downstream of receptor activation. (A) pMad (red and upper inset) and *H15*-lacZ (green and lower inset) staining detected by anti-pSmad1/5/8 and anti-β-galactosidase antibody on a third instar leg imaginal disc (dorsal up). *H15*-lacZ is used as a marker for the mid domain. *mid* and *H15* are redundant T-box genes and are co-regulated and co-expressed (Svendsen et al., 2009, 2015). (B, C) Loss-of-function clones for mid^{1a5} $H15^{x4}$ (absence of GFP, green) stained for pMad in third instar leg discs. Arrowheads show increased pMad staining in clones (B, C; red and single channel) and expanded pMad staining as seen in (C). (D, E) Gain-of-function clones (expressing GFP, green) stained for pMad in third instar leg discs. (D) *Ay*Gal4 clones expressing UAS-tkv^{QD} UAS-*GFP* show increased pMad staining (nuclear, red and single channel). (E) Decreased levels of pMad (note decreased nuclear pMad stain) are seen with co-expression UAS-$mid^{2.8}$ (mid^{+}); UAS-tkv^{QD} in *Ay*Gal4 clones (red and single channel). (F, G) Gain-of-function clones in third instar leg discs (expressing GFP, green) are stained with an antibody that recognizes all forms of Mad. (F) *Ay*Gal4 clones expressing UAS-tkv^{QD} UAS-*GFP*, show nuclear localization of Mad (red and single channel). (G) With co-expression of UAS-mid^{+}; UAS-tkv^{QD} in *Ay*Gal4 clones, Mad is cytoplasmic and levels are not reduced compared to adjacent GFP-negative cells.

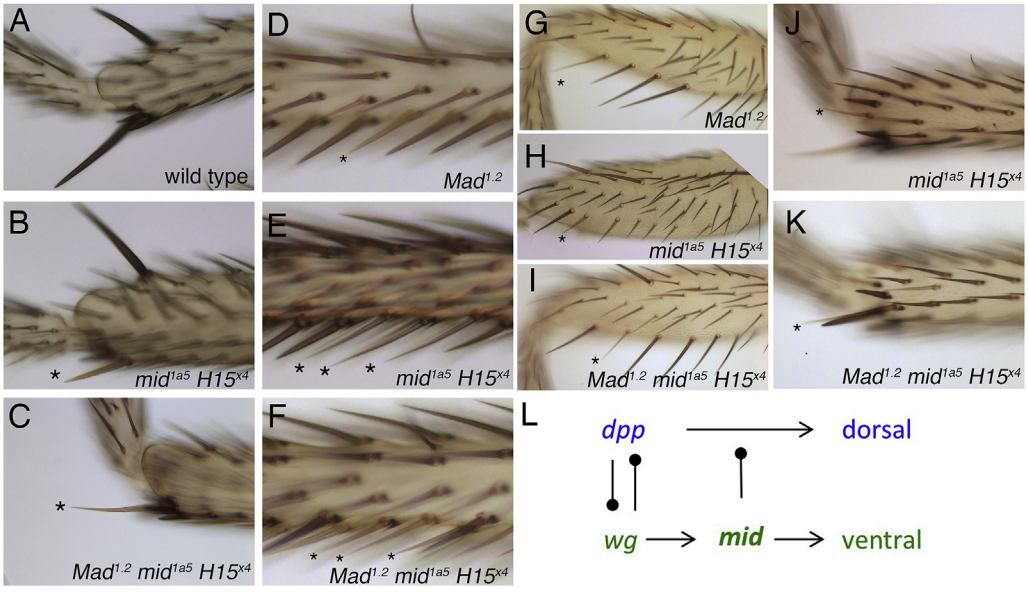

Fig. 3. $Mad^{1.2}mid^{1a5}H15^{x4}$ double mutant phenotypes. (A) Wild type second leg basitarsus and distal tibia (distal left, dorsal up). Loss-of-function clones, *y*, are marked with asterisks: (B) ventral mid^{1a5} $H15^{x4}$ mutant clone marked with *y* showing transformation of AB to a PAB-like bristle; (C) $Mad^{1.2}$ mid^{1a5} $H15^{x4}$ mutant clone showing the formation of an AB-like bristle; (D) $Mad^{1.2}$ clone marking a row 1/8 bristle maintains peg-shape; (E) mid^{1a5} $H15^{x4}$ clone transforming row 1/8 bristles from peg to rapier-shape characteristic of dorsal row 4/5 bristles; (F) a $Mad^{1.2}$ mid^{1a5} $H15^{x4}$ clone transforms row 1/8 bristles from a peg to a rapier-shape; (G) $Mad^{1.2}$ clone marking a ventral femur bristle; (H) mid^{1a5} $H15^{x4}$ clone transforming several ventral femur bristles to shorter bristle type; (I) $Mad^{1.2}$ mid^{1a5} $H15^{x4}$ clone also transforms ventral femur row to a shorter non-ventral bristle type; (J) mid^{1a5} $H15^{x4}$ clone transforms a spur bristle to a more lateral type of bristle as does a (K) $Mad^{1.2}$ mid^{1a5} $H15^{x4}$ clone; (L) Genetic pathways in the ventral leg. *mid* inhibits the promotion of a dorsal fate by *dpp* in the ventral leg as indicated by the epistasis of *Mad* over *mid H15* in AB development. *Mid H15* must also promote ventral fate as indicated by the failure of $Mad^{1.2}$ mid^{1a5} $H15^{x4}$ mutants to rescue most ventral structures.

should be rescued to ventral fate when they also lack *Mad*. $Mad^{1.2}$ mutant clones induced in second instar or early third instar had no effect on ventral structures such as the AB, spurs, row 1/8 bristles, sex combs or ventral femur bristles. In contrast, in dorsal regions of the leg, $Mad^{1.2}$ defects such as reduction in size of dorsal row bristles, dorsal joint loss, and cuticle inclusions inside the leg were observed frequently. This is consistent with previous work demonstrating that loss of Dpp does not affect ventral fate (Held and Heup, 1996). Clones mutant for $Mad^{1.2}$ mid^{1a5} $H15^{x4}$ rescued the effects on AB development seen in mid^{1a5} $H15^{x4}$ clones. The AB is a long mechanosensory bristle located at the ventral distal apex of the tibia on the second leg. It lacks a bract and is located distal to a cluster of 5–6 peg-shaped bristles called spurs (Fig. 3A). In mid^{1a5} $H15^{x4}$ mutant clones, the AB is shorter and located proximal to the spur bristles and thus resembles the dorsal PAB in size and location along the P/D axis (Fig. 3B) (Svendsen et al., 2009). In $Mad^{1.2}$ mid^{1a5} $H15^{x4}$ clones, the AB maintains its length, lack of bract, and apical position distal to the cluster of spurs and thus appears ventral in fate (Fig. 3C). This indicates that *mid H15* function to block the effects of Dpp signaling in the AB primordium and suggests that ventral is the default fate for the AB that occurs in the absence of Dpp signaling.

In contrast, no other structures were restored to ventral fate in the $Mad^{1.2}$ mid^{1a5} $H15^{x4}$ mutant clones. The row 1/8 bristles that run along the ventral surface of the second leg have a characteristic peg-shape. Bristles in the dorsal 4/5 rows and lateral 2/7 and 3/6 rows are rapier-shaped with the dorsal row 4/5 bristles being longer than those in the lateral rows. $Mad^{1.2}$ clones in row 1/8 are normal (Fig. 3D), $H15^{x4}$ mid^{1a5} mutant row 1/8 bristles are transformed into long rapier shaped bristles similar in size and morphology to the row 4/5 bristles typically seen on the dorsal side (Fig. 3E) (Svendsen et al., 2009). In $Mad^{1.2}$ $H15^{x4}$ mid^{1a5} clones located in row 1/8, the bristles are transformed from peg to rapier-shaped, although the triple mutant clones are shorter, suggesting they may not be ventral or dorsal, but perhaps lateral in fate (Fig. 3F). A series of large bristles on the ventral surface of the dorsal femur are much smaller in the absence of *mid H15* function (Fig. 3H) but do not require Mad (Fig. 3G). These remain small in the triple mutant clones (Fig. 3I). Similarly, the spurs associated with the AB are transformed to a rapier-shape characteristic of more lateral tibia bristles (Fig. 3J and K), and the first leg sex comb bristles and transverse bristle rows are lost in both *mid H15* and *Mad mid H15* genotypes (not shown), again indicating no rescue of the *mid H15* phenotype. The failure of the absence of *Mad* to rescue the dorsalization of these ventral structures by *mid H15* loss-of-function indicates that the T-box genes are required to promote these particular ventral fates, even in the absence of the Dpp signal. Thus, throughout most of the ventral domain of the disc, *mid* does not simply repress a default Dpp-dependent dorsal fate but must also actively promote ventral fate independent of inhibiting Dpp (Fig. 3L).

3.4. *mid and H15 repress downstream target genes in the ventral leg*

How are these two pathways, the inhibition of Dpp and the Dpp-independent specification of ventral fate, reflected in Mid transcription factor function? In order to address this, we looked at the regulation of several genes expressed in the leg imaginal disc. We have shown previously that Mid acts as a repressor for genes in embryo and leg development, including negative feedback on its own expression in the leg imaginal disc (Buescher et al., 2004; Svendsen et al., 2009, 2015). Mid represses genes by recruiting the co-repressor Groucho (Gro) through the eh1 domain, which promotes inhibitory chromatin states. The inhibition of Dpp signaling suggests that Mid may also repress Dpp target genes. We examined the effects of loss-of-function for *mid H15* on the expression of a lacZ enhancer-trap inserted in the Dpp-target gene *Daughters-against-decapentaplegic (Dad*-lacZ*)* (Tsuneizumi et al., 1997). The *Dad*-lacZ reporter is expressed broadly along the A/P boundary, with higher levels in the dorsal half of the leg imaginal disc (Fig. 4A). In the ventral *Dad* expression domain, *mid H15* mutant clones consistently show a cell-autonomous increase in expression indicating that the inhibition of Dpp signaling by *mid H15* function can also be demonstrated at the level of Dpp-target gene readout (Fig. 4B). All *mid H15* mutant clones that overlap the ventral domain have increased in *Dad*-lacZ expression (21/21), while none of the clones in the dorsal or lateral domains do (0/8). We also tested whether *mid*-expressing cells repress *Dad*-lacZ expression. We observed a weak cell-autonomous reduction of *Dad*-lacZ expression in half of the clones (8/16) expressing a UAS-mid^{+} transgene (Fig. 4C,E). The relatively weak repression is not surprising given that loss-of-function for *mid H15* causes only a modest increase in *Dad*-lacZ expression levels. We then made use of UAS-mid^{eh1}, which has a F41E substitution in the engrailed-homology-1 (eh1) domain. The UAS-mid^{eh1} transgene is defective in gene repression due to decreased Groucho co-repressor binding but is still able to bind DNA and other Mid binding partners (Formaz-Preston et al., 2012). In gain-of-function experiments, we used a strain with two UAS-mid^{+} insertions that results in an expression level that is 50% of UAS-mid^{eh1} (Fig S3A,B). We found that the ability of UAS-mid^{eh1} to repress *Dad*-lacZ was reduced compared to wildtype with only a small number of clones (2/17) having decreased *Dad*-lacZ repression (Fig. 4D and E). This suggests that Mid repressor function is required for the repression of *Dad*, consistent with Mid being a direct repressor of *Dad*. In support of direct regulation of *Dad* by Mid, we found binding of Mid to *Dad* enhancers in chromatin-immunoprecipitation assays (ChIP). In PCR-ChIP, a Flag-tagged Mid protein was enriched at a *Dad* enhancer in ventral leg imaginal disc chromatin (Fig S3C,D). Thus, in addition to antagonizing Dpp signaling in the leg, Mid also represses Dpp target genes, in an apparently direct manner.

Another role for *mid H15* function may be to antagonize a default lateral fate. Previous work (Held et al., 1994) has suggested that lateral may be the default fate in the D/V axis because flies doubly mutant for *wg* and *dpp* hypomorphic alleles formed lateral structures at the expense of dorsal and ventral elements. Our results show that some ventral structures developed as non-dorsal and non-ventral in *Mad mid H15* mutant clones, supporting the possibility for a default lateral fate in the D/V axis. Given these results, we wished to test whether *mid H15* function is required to repress lateral genes. P-element reporters inserted in the *Unpaired* locus are known to be expressed in lateral domains (Ayala-Camargo et al., 2007; Sun et al., 1995). We tested whether *mid H15* were required to repress the expression of the *Unpaired*-lacZ *(Upd*-lacZ*)* reporter. *Upd*-lacZ is expressed in two lateral domains, one each in the anterior and posterior halves of the leg imaginal disc. Double labeling for *Upd*-lacZ and *H15* shows that the ventral boundaries of the two *Upd*-lacZ expression domains align perfectly with the boundaries of H15 expression (Fig. 4F). This boundary has previously been shown to be controlled by Wg repression (Ayala-Camargo et al., 2007). Thus, it is possible that Wg activation of *mid H15* leads to repression of the *Upd* genes in the ventral region of the disc. Consistent with Mid repression of *Upd* genes, there is ectopic cell-autonomous activation of *Upd*-lacZ in *mid H15* mutant clones located ventrally (Fig. 4G). In gain-of-function, the majority (23/24) of UAS-mid^{+} expressing clones repress *Upd*-lacZ (Fig. 4H,J) and this is decreased in clones expressing the mid^{eh1} transgene (9/20) (Fig. 4I and J). The *Upd* locus contains three genes encoding Jak/Stat pathway ligands (*Upd1, Upd2, Upd3*). In an unpublished ChIP-seq experiment, we identified a strong Mid signal upstream of *Upd3* and find that we are able to validate binding of Flag-Mid to this sequence in PCR-ChIP assays (Fig S3E,F). The reduced repression of *Upd*-lacZ by UAS-mid^{eh1} expression and the localization of Flag-Mid to a putative regulatory region of *Upd3* suggest that Mid is a direct repressor of lateral *Upd* expression. Thus, *mid H15* may also function in the repression of a default lateral fate.

The ability of *mid H15* to promote ventral fate independent of repressing Dpp-signaling means that Mid must regulate additional ventral gene expression. However, to date we have not found evidence for a ventral gene directly activated by Mid. We tested two ventral specific transcription factors, *gooseberry neuro (gsb-n)* (Zhang et al., 1994) (Fig S4A) and *ladybird-early (lbe)* (Jagla et al., 1997) (Fig S4E) and found

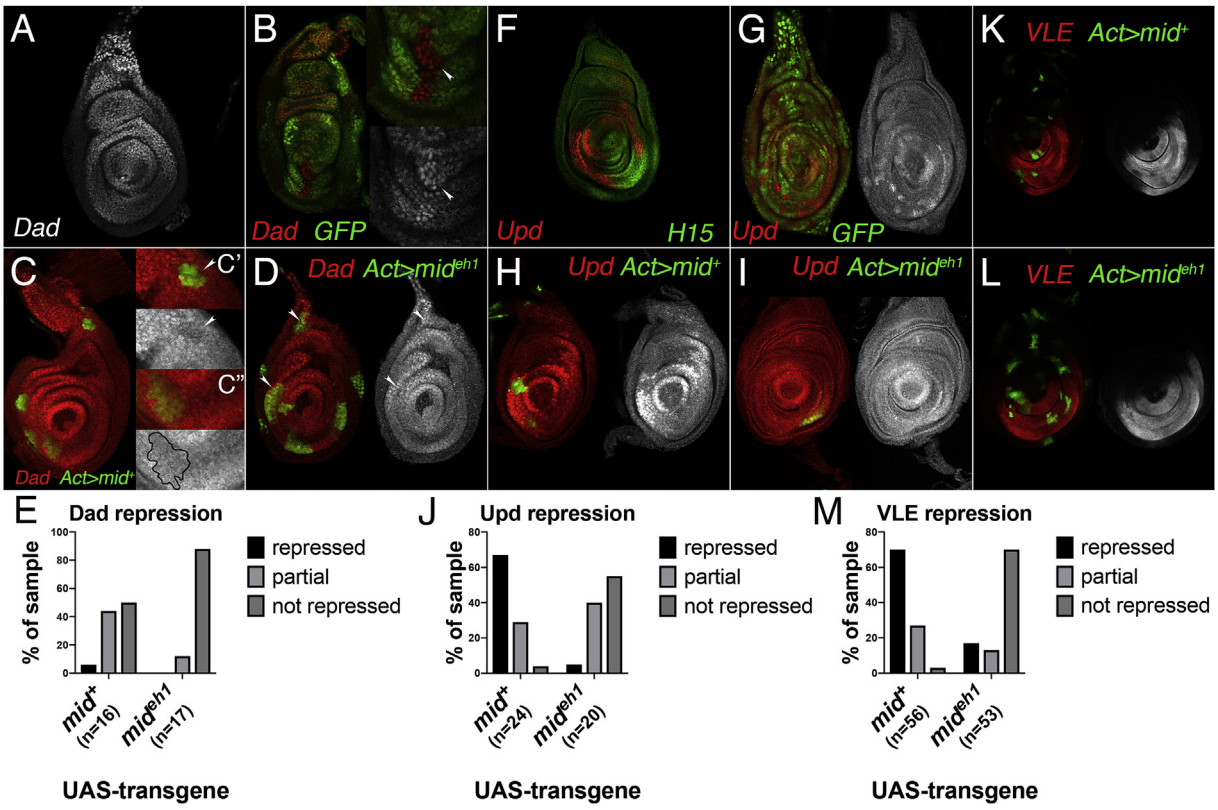

Fig. 4. *mid*$^{+}$ represses genes in the ventral domain in an eh1 dependent manner. (A) *Dad*-lacZ is expressed in dorsal and ventral *dpp* domains, expression is highest dorsally. (B) *mid*^{1a5} *H15*^{x4} loss-of-function clones (absence of GFP, green) have increased expression of *Dad*-lacZ (arrowhead, red and single channel). (C) *Ay*Gal4 clones expressing UAS-Flag-*mid*$^{wt9b+8a}$ (*mid*$^{+}$, GFP, green) and stained for *Dad*-lacZ (red). Insets show a repressed clone (arrowhead in C′ red and single channel) and a partially repressed clone (outlined in single channel, C″). (D) *Ay*Gal4 clones expressing UAS-*mid*^{eh1}. These clones rarely repress *Dad*-lacZ (arrowhead, red and single channel). A summary of the percent repression by UAS-*mid*$^{+}$ and UAS-*mid*^{eh1} is shown in (E). (F) The complementary expression patterns of lateral *Upd*-lacZ, a reporter for the *Upd* locus (red) and ventral H15 protein (green). (G) Ventrally located *mid*^{1a5} *H15*^{x4} loss-of-function clones (absence of GFP, green) have increased or ectopic expression of *Upd*-lacZ (red, single channel). (H) *Ay*Gal4 clone expressing UAS-*mid*$^{+}$ (UAS-*GFP*, green) and *Upd*-lacZ (red). Almost all clones are completely or partially repressed (Graph, J). (I) *Ay*Gal4 clone expressing UAS-*mid*^{eh1}, UAS-*GFP* (green); *Upd*-lacZ (red). Most *mid*^{eh1} clones show little or no repression of *Upd*-lacZ (Graph, J). (K) *Ay*Gal4 clone expressing UAS-*mid*$^{+}$ and UAS-*GFP* (green) and showing *VLE*-lacZ expression at the ventral portion of the leg disc (red); single channel *VLE*-lacZ with suppressed clones. (L) *Ay*Gal4 clone expressing UAS-*mid*^{eh1}, UAS-*GFP* (green); *VLE*-lacZ (red); single channel shows *VLE*-lacZ, most clones are not suppressed. (M) Frequency of *mid*$^{+}$ and *mid*^{eh1} expressing clones that repressed or partially repressed *VLE*-lacZ.

they were both activated by Wg signaling (Fig S4B,C,F,G) but neither were lost in *mid H15* mutant clones (Fig S4D,H). We showed previously that *mid* and *H15* were required for the activation of *Sex combs reduced* (*Scr*) expression in the ventral leg (Svendsen et al., 2009). *Scr* is required for the formation of the ventral sex comb and transverse row bristles on the first leg. However, it is likely that *mid H15* regulation of *Scr* is indirect. In gain-of-function experiments, some UAS-*mid*$^{+}$ expressing clones can increase or induce ectopic Scr (Fig S4I) but UAS-*mid*^{eh1} clones do not affect *Scr* expression (Fig S4J). Therefore, it is likely that Mid induces *Scr* indirectly by repressing a *Scr*-repressor. However, *mid H15* do act as feedback inhibitors of their own expression. Increasing the levels of either gene represses the other and vice versa. *mid* and *H15* repress the expression of *VLE*, an enhancer in the *mid* 3′-regulatory region. (Svendsen et al., 2015). In gain-of-function experiments, most clones expressing UAS-*mid*$^{+}$ decreased or repressed *VLE*-lacZ expression (Fig. 4K,M) while clones of cells expressing UAS-*mid*^{eh1} were compromised for *VLE*-lacZ repression (Fig. 4L and M). As we have shown for *Dad* and *Upd*, we find that Flag-Mid binds to VLE sequences in PCR-ChIP assays in ventral leg imaginal disc chromatin (Fig S3G,H). Thus, the negative feedback of Mid on its own transcription is also likely direct.

3.5. *mid*^{eh1} *is compromised for the induction of ectopic dorsal fate*

The repressor defective *mid*^{eh1} mutant allele is clearly compromised for target gene repression in the ventral leg, suggesting that repression is an essential role for Mid. Here we ask what effect the *mid*^{eh1} mutation has in ventral leg development. We first expressed the *UAS-mid*^{eh1} transgene in dorsal cells and assessed the effects on dorsal to ventral transformation. Ectopic UAS-*mid*$^{+}$ under the control of *dpp*Gal4 causes an extreme dorsal to ventral transformation, which includes loss of virtually all dorsal structures and replacement with a mirror image of ventral structures (Fig S5A). Analysis of gene expression in *dpp*Gal4>UAS-*mid*$^{+}$ imaginal discs show that this phenotype is associated with the complete repression of *omb*-lacZ in the dorsal leg (Fig S5D), and ectopic expression of endogenous *wg* in the dorsal cells of the leg imaginal disc (Fig S5G). In contrast, less than 1% of *dpp*Gal4>UAS-*mid*^{eh1} legs show any dorsal defects (Fig S5B). Similarly, UAS-*mid*^{eh1} does not repress *omb* (Fig S5E) or cause ectopic expression of *wg* (Fig S5H). Ectopic expression of *wg* in the dorsal domain has a similar effect on dorsal ventral patterning and gene expression to the effects of ectopic UAS-*mid*$^{+}$ seen here (Brook and Cohen, 1996; Jiang and Struhl, 1996; Johnston and Schubiger, 1996; Theisen et al., 1996). Thus, our results suggest that the *dpp*Gal4>UAS-*mid*$^{+}$ induced transformation to ventral fate is an all-or-none phenotype caused by the repression of dorsal genes by transgenic UAS-*mid*$^{+}$. This results in the de-repression of *wg* in the dorsal region, thereby activating the rest of the endogenous ventral gene expression program.

In order to assess the effects of ectopic UAS-*mid*$^{+}$ without the downstream activation of *wg*, we used a different dorsal driver (*omb*-Gal4). Ectopic expression of UAS-*mid*$^{+}$ in the *omb* domain

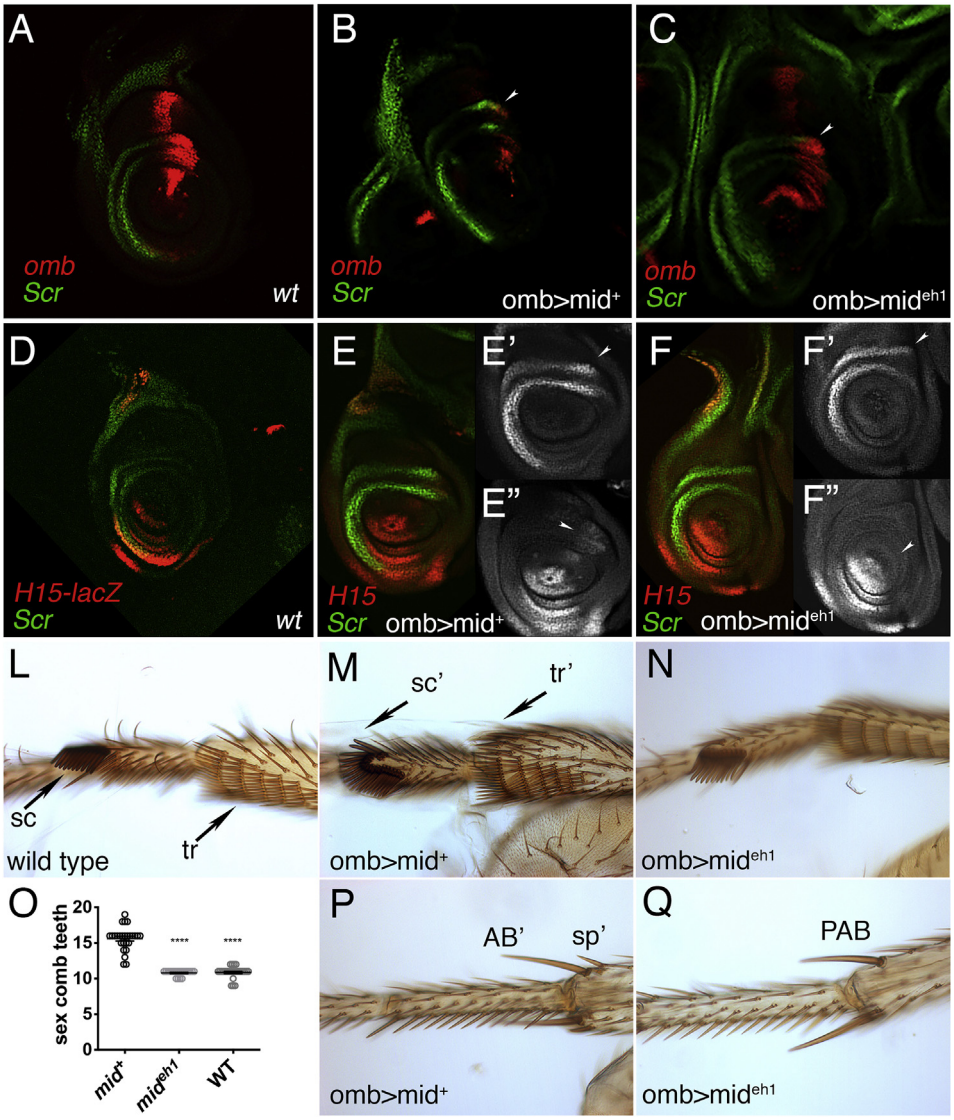

Fig. 5. *mid*^{eh1} is defective in dorsal to ventral transformation. (A) WT expression patterns of *omb* and *Scr* (*omb*-lacZ, red, Scr protein, green). The effects of *mid* transgene expression on *Scr*, *omb* and *H15* are shown in panels B–F. (B) *omb*-Gal4, expressed in the dorsal domain of the leg imaginal disc, was used to drive expression of UAS-*mid*$^{+}$ (Flag-*mid*$^{wt8a+9b}$ throughout this figure) or UAS-*mid*^{eh1}. UAS-*mid*$^{+}$ causes ectopic expression of Scr in the *omb* domain (an extension of the arc, green, running ventral to dorsal (B, arrowhead). (C) Little if any ectopic Scr is seen with UAS-*mid*^{eh1} expression in the *omb* domain (arrowhead). Similarly, *omb*-lacZ (red) expression is greatly reduced by UAS-*mid*$^{+}$ (red in B) but is not reduced by UAS-*mid*^{eh1} expression in the *omb* domain (red in C). (D) A control leg disc stained for Scr and H15 protein expression (anti-Scr, green, and anti-NMR1 antibodies to H15, red). *omb*Gal4 was again used to drive expression of UAS-*mid*$^{+}$ (E) and UAS-*mid*^{eh1} (F). UAS-*mid*$^{+}$ discs have weak ectopic H15 expression (red) in the *omb* domain (arrowhead in single channel, E″). Ectopic Scr expression is also highlighted (green, arrowhead in single channel, E′). (F) *omb*-Gal4>UAS-*mid*^{eh1} discs do not show any ectopic H15 (red, arrowhead in single channel F″) or Scr (green, and arrowhead in single channel, F′) in the *omb* domain. (L) Wild type first leg basitarsus and distal tibia. Arrows denote ventral pattern bristles (sex comb, on basitarsus, left and transverse rows, on tibia, right). (M, N) First leg cuticle of flies with overexpression of UAS-*mid*$^{+}$ and UAS-*mid*^{eh1} in the *omb* domain; (M) Ectopic expression of UAS-*mid*$^{+}$ with *omb*Gal4 causes expansion of ventral pattern elements like sex comb (sc', arrow) and other ectopic ventral pattern elements (transverse rows, tr', arrow) on the dorsal leg; (N) with ectopic UAS-*mid*^{eh1} expression, the sex comb and transverse rows are not expanded dorsally. (O) Graph summarizing sex comb bristle numbers in *omb*-Gal4 driving UAS-*mid*$^{+}$ and UAS-*mid*^{eh1} legs (M,N). Statistics used are Tukey's multiple comparisons test (comparing to mid^{+}), with bars representing standard deviation, significance is indicated, * (P value 0.01 to 0.05, significant) and ****(P value < 0.0001, extremely significant). (P, Q) show cuticle from second legs with in UAS-*mid*$^{+}$ or UAS-*mid*^{eh1} over expression by the *omb*Gal4 driver (P) Ectopic UAS-*mid*$^{+}$ causes transformation of dorsal PAB to more distal AB-like bristle (AB′). Ectopic spur (sp') is also present. (Q) Legs with ectopic UAS-*mid*^{eh1} have dorsal cuticle on second leg that is essentially WT.

(*omb*Gal4>UAS-*mid*$^{+}$) induces a dorsal to ventral transformation that is weaker than that caused by the *dpp*Gal4 driver. *omb*-lacZ is only slightly decreased (Fig S5I,J) and Wg is not ectopically expressed (Fig S5L,M). However, ectopic UAS-*mid*$^{+}$ expression driven by *omb*Gal4 does induce the ventral genes *Scr* and *H15*. In first leg imaginal discs, *Scr* is expressed at high levels in two arcs that extend from the ventral most tibia and tarsal regions to the dorso-lateral region of the disc stopping adjacent to the *omb* expression domain (Fig. 5A). Ectopic UAS-*mid*$^{+}$ expression in the *omb* domain induces ectopic Scr expression in the *omb* domain but the ectopic expression is restricted to cells at the same proximal-distal position as the tibia and tarsus arcs (Fig. 5B,E) (Svendsen et al., 2009). Ectopic UAS-*mid*$^{+}$ in the *omb* domain also induces ectopic H15 throughout the distal part of the *omb* domain (Fig S5L, Fig. 5E). The induction of both Scr and H15 is not seen when UAS-*mid*^{eh1} is expressed in the *omb* domain (Fig S5M, Fig. 5F).

Analysis of the adult cuticle shows that UAS-*mid*^{eh1} is compromised for the induction of ventral structures. On the first leg, the transverse rows (Fig. 5L) are closely packed bristles that arise in positions anterior to the ventral midline of the distal tibia and basitarsus in the first leg. In the male first leg, the distal-most transverse row is modified to form sex combs: dark, thicker, curved and easily scored bristles (Fig. 5L). Ectopic expression of UAS-*mid*$^{+}$ in the dorsal domain with *omb*Gal4 resulted in the induction of sex comb bristles and transverse rows in dorsal cells (Fig. 5M). The mean number of sex comb bristles (15.6) was increased compared to controls (10.9 sex comb teeth) (Fig. 5O). Formation of ectopic sex combs was suppressed (10.8) and ectopic transverse row bristles also failed to form when UAS-*mid*^{eh1} was expressed dorsally (Fig. 5N and O). These results are consistent with the observed effects on

Scr expression observed in UAS-*mid*$^{+}$ compared to UAS-*mid*^{eh1}. In the second leg, ectopic UAS-*mid*$^{+}$ expression under the control of *omb*Gal4 induces ectopic AB in place of the normal PAB in all legs (Svendsen et al., 2009) (Fig. 5P). The normal AB is associated with 5–6 spurs arranged proximally and ectopic *mid*$^{+}$ is able to induce ectopic spurs in all legs (mean# of spurs = 2.1) (Fig. 5P). UAS-*mid*^{eh1} failed to induce ectopic AB or spurs (Fig. 5Q).

3.6. Rescue of mid H15 loss-of-function by mid^{eh1} mutants

The ectopic expression experiments showed that UAS-*mid*^{eh1} is compromised for all of the gain-of-function effects in the dorsal leg. However, the interpretation of the role of UAS-*mid*$^{+}$ and UAS-*mid*^{eh1} is complicated by the induction of *wg* and/or *H15* expression in dorsal cells. Furthermore, the presence of high levels of Dpp signaling in the dorsal most cells also complicates the interpretation of the inability of UAS-*mid*^{eh1} to promote ventral fate because the antagonism between Mid and Dpp may exacerbate the effects of the *mid*^{eh1} mutation. In order to more clearly assess the consequences of *mid*^{eh1}, we tested its ability to rescue ventral cells mutant for *mid H15*. We used the MARCM system (Lee and Luo, 1999) which allows the activation of UAS-transgenes in mutant cells. We expressed the control UAS-*mid*$^{+}$ transgene under *tub*Gal4 control in *mid H15* clones marked by the absence of the cuticle marker *yellow*$^{+}$ (*y*$^{+}$). In MARCM rescue experiments, we used a strain with a single UAS-*mid*$^{+}$ insertions that results in an expression level that is 30% of UAS-*mid*^{eh1} (Fig S3A,B). UAS-*mid*$^{+}$ was able to reliably rescue *mid H15* ventral defects in row 1/8, sex combs, spurs, and apical bristles.

The rescue of the *mid*^{1a5} *H15*^{x4} AB to PAB transformation in *Mad*$^{1.2}$ *mid*^{1a5} *H15*^{x4} clones (Fig. 3C) suggests that, in the AB, *mid H15* may only function to repress the effects of Dpp signaling that would otherwise transform the structure to the dorsal PAB fate. To assess the rescue of AB by UAS-*mid*^{eh1}, we scored clones that had yellow bristles both distal and proximal of the location of the AB. Both UAS-*mid*$^{+}$ and UAS-*mid*^{eh1} showed variable rescue of the AB bristle size. *mid*^{1a5} *H15*^{x4} mutant cells expressing UAS-*mid*$^{+}$ rescued the AB to PAB transformation in all cases (11/11), with an AB-like bristle, meaning a larger bristle lacking a bract and located distal to the spur bristles near the apex of the tibia. Almost half of these (5/11) were shorter than WT (Fig 6A,C). UAS-*mid*^{eh1} had a

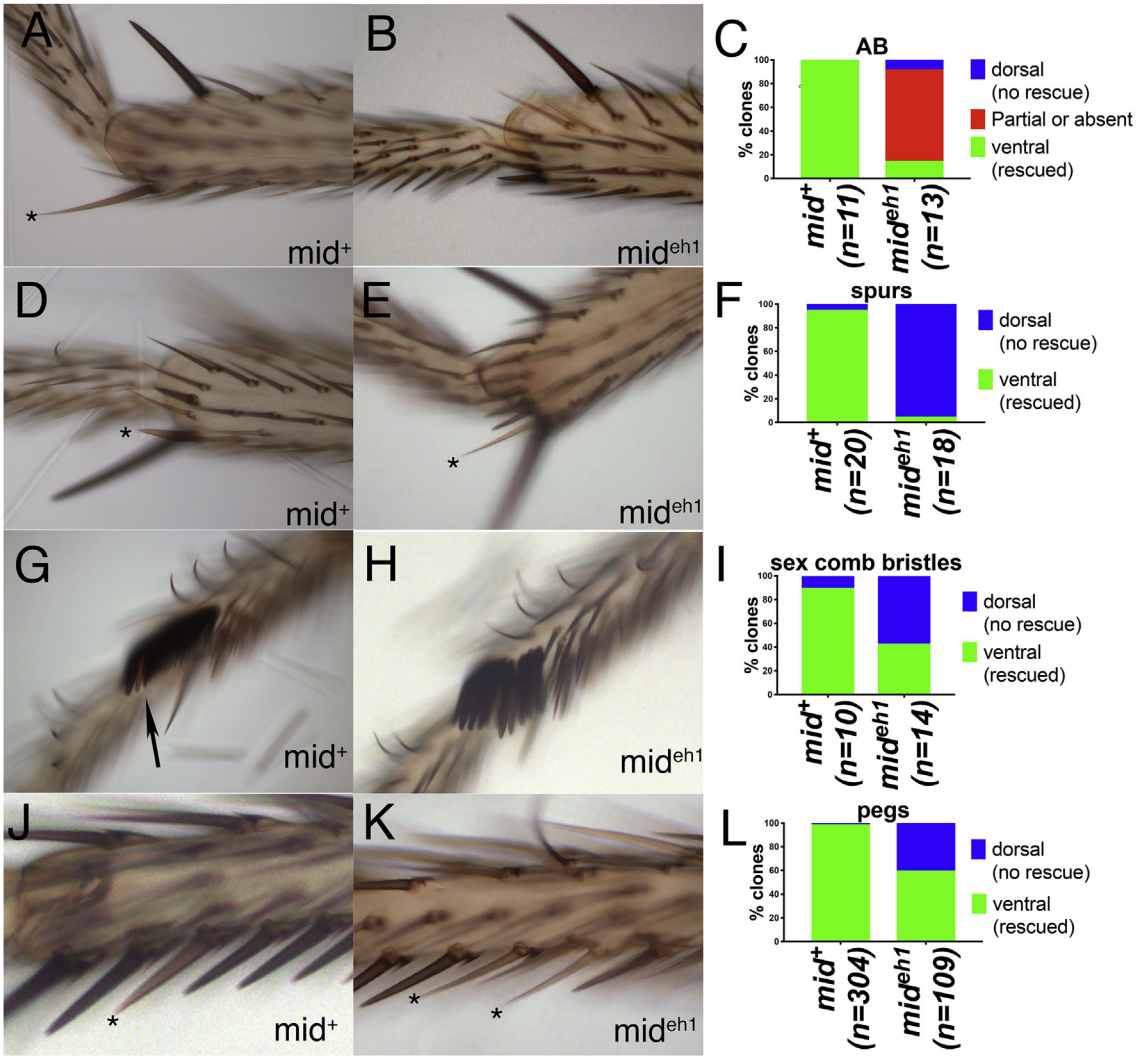

Fig. 6. MARCM rescue of *mid*^{1a5} *H15*^{x4} mutant clones. Cuticle images showing *mid*^{1a5} *H15*^{x4} clones marked with *y* with rescuing transgenes indicated. (A) UAS-*mid*$^{+}$ (UAS-Flag-*mid*^{wt8a} in this figure) rescues the AB in this second leg clone (asterisk, note distal position) while in (B) AB is missing in a clone expressing UAS-*mid*^{eh1}. (D) UAS-*mid*$^{+}$ rescues most spur bristle clones (asterisk) but (E) UAS-*mid*^{eh1} fails to rescue the spur clone (asterisk, note long, thin rapier-like bristle). (G) UAS-*mid*$^{+}$ rescues a sex comb clone (arrow). (H) Sex comb showing failure of UAS-*mid*^{eh1} expressing clone to rescue (gap). (J and K) show *y* marked clones (asterisks) in the 1/8 peg rows on second leg basitarsus. (J) MARCM rescue by UAS-*mid*$^{+}$ gives wild type peg bristles (note peg morphology and wild type length of the rescued bristle, asterisk). (K) *y* 1/8 row bristle clones are not rescued by UAS-*mid*^{eh1} and retain the rapier phenotype of *mid*^{1a5} *H15*^{x4} mutants (see also Fig. 3E). Graphs (C, F, I, L) indicate percentage of MARCM clones showing rescue of ventral structures by UAS-*mid*$^{+}$ or UAS-*mid*^{eh1}.

reduced ability to promote AB formation. The majority of the clones have either no rescue, an ambiguous partial rescue phenotype with a partially distalized bristle, in line with the spurs, or are missing the AB altogether (Fig. 6B and C). Taken together with the *Mad mid H15* results, this suggests that the repression of Dpp pathway genes by Mid is essential for AB development.

We saw a similar strong dependence on eh1 function in the spur bristles. In MARCM rescue clones, UAS-mid^{+} had near complete rescue of spurs (19/20), while UAS-mid^{eh1} was largely unable to rescue the wild type phenotype (1/18) (Fig. 6E and F). In sex combs and row 1/8 bristles, UAS-mid^{eh1} was able to partially rescue the *mid H15* mutant phenotype. To score the rescue of sex comb bristles in the MARCM experiment, we counted the number of sex combs with obvious gaps as not rescued and those with sex comb teeth marked *yellow* as rescued. UAS-mid^{+} rescued most sex combs to wild type (9/10) (Fig. 6G,I) while UAS-mid^{eh1} rescued almost half of the clones (6/14) (Fig. 6H and I). Similar results were seen in rescue of the row 1/8 bristles. UAS-mid^{+} rescued almost all row 1/8 bristles to wild type (99%) (Fig. 6J,L). UASmid^{eh1} rescued more than half of the bristles (59%) (Fig. 6K,L).

4. Discussion

The development of the D/V axis of the fly leg is orchestrated by dorsal Dpp and ventral Wg, which induce downstream T-box transcription factors, *omb* and *Doc* in dorsal cells (Weiss et al., 2010), and *mid H15* in ventral cells, respectively (Svendsen et al., 2015). Wg and Dpp maintain their expression through a complex pathway of mutual repression. Studies manipulating D/V pathway gene expression have shown that the pathway involves mutual repression of *wg* and *dpp* gene expression, repression of each other's downstream target genes, feedback by the target genes to repress *wg* and *dpp*, and also repression between dorsal and ventral target genes (Estella et al., 2012). The mutual inhibition between the two groups of genes complicates the study of D/V axis patterning because gain-of-function for a gene in one group necessarily leads to decreased or loss of expression of the other group of genes. Thus, it has been difficult to dissect exactly what Wg, Dpp, and their downstream genes do in D/V patterning, other than repress the other group (Brook, 2010). The cell autonomy of the *mid H15* ventral to dorsal transformation, occurring in the absence of ectopic expression of *Dpp*, *omb* (Svendsen et al., 2009) or *Doc* (unpublished) indicated that *mid H15* are not simply part of the D/V cross-repression network. Instead, it suggested that a critical event downstream of Dpp and Wg in dorsal/-ventral patterning is the expression of *mid H15* in ventral cells. *mid H15* act as an essential genetic switch, triggering ventral patterning. In this study, we show that *mid H15* function in an inhibitory pathway that antagonizes Dpp signaling as well as a Dpp-independent pathway that specifies ventral fate.

One role for *mid H15* in ventral fate specification is to antagonize the effects of the dorsal Dpp signal in the ventral leg. Remarkably, one mechanism is through inhibition of pMad levels. Clones of *mid H15* mutant cells have increased levels of pMad detected with a phospho-specific antibody, and ectopic Mid decreases pMad in ectopic sites when Dpp signaling is activated by expressing an activated receptor (UAS-tkv^{QD}). Thus, Mid and H15 apparently decrease Dpp signaling in the cell downstream of receptor activation. How do Mid and H15 regulate pMad levels? One possibility is by regulating the expression of any of several genes expressed in the leg imaginal disc that either promote or inhibit pMad accumulation. These include genes that regulate pMad nuclear export (Zeng et al., 2007), de-phosphorylation (Chen et al., 2006; Urrutia et al., 2016), and stability (Chen et al., 2010; Takaesu et al., 2006). We note that a similar effect has been reported in the eye imaginal disc, where the transcriptional co-repressor Ctbp is required to repress pMad levels suggesting that transcriptional control of pMad regulators may be common (Eusebio et al., 2018). Other T-box factors have also been reported to inhibit BMP signaling. In mouse, Tbx20, the *mid H15* homolog, and Tbx1 have both been shown genetically to antagonize BMP activated genes. For instance, Tbx20 is required to repress Tbx2, the *omb* homolog, to allow chamber formation in heart development (Stennard et al., 2005). In cell culture, Tbx20 and Tbx1 have been shown to inhibit BMP target gene expression by binding to Smad1, the Mad homolog, thus blocking target gene activation (Fulcoli et al., 2009; Singh et al., 2009). However, there is no evidence in those systems that T-box interactions decrease pSmad1 levels. Nonetheless, the parallels between the two systems are intriguing and suggest that tissue specific inhibition of BMP signaling by T-box transcription factors is conserved.

Our results suggest that *mid H15* function interferes with the Dpp pathway in a coordinated manner because in addition to modulating Dpp pathway activity, they also repress the Dpp-target gene *Dad*. The expression of *Dad*, a well characterized Dpp target gene (Weiss et al., 2010), is upregulated in *mid H15* mutant clones and Mid is detected at *Dad* enhancers in ChIP assays on leg imaginal disc chromatin. This is consistent with Mid being a transcriptional repressor of *Dad*. Does Mid regulate other Dpp target genes? This seems likely, however, not all Dpp target genes respond to changes in *mid* function in the same manner. While *mid* is necessary and also weakly sufficient to repress *Dad*, we previously found that *mid* is sufficient but not necessary to repress *omb*. Unlike *Dad, omb* is not upregulated in *mid H15* loss-of-function clones (Svendsen et al., 2009). What could account for this difference? The lack of *omb* expression in response to the lower levels of Dpp signaling in the ventral leg may indicate that *omb* requires a higher threshold of Dpp signaling for activation compared to *Dad*. It may be that the increased Dpp signaling in *mid H15* clones is still insufficient to activate *omb*. It may also be that there are redundant repressors of *omb* in the ventral leg such as Wg signaling or Wg-target genes, such as *lbe* and *gsb-n*, which could act in parallel to repress *omb*. Finally, the effects of *mid* expression to repress *omb* could be truly gain-of-function. Mid may have no normal role repressing *omb* in the ventral leg but is able to block *omb* expression as a result of the inhibition of Dpp signaling that occurs when *mid* is expressed ectopically in the *omb* domain. Further analysis of *Dad, omb,* and other genes regulated by Mid and Dpp signaling will be necessary to distinguish between these possibilities.

mid H15 are also required for ventral fate specification beyond antagonizing the Dpp pathway and target genes. Most transformed ventral structures were not rescued in cells null for *mid H15* and mutant for $Mad^{1.2}$, which blocks Dpp signaling (Wiersdorff et al., 1996). Some resulting phenotypes, in the spurs and sex combs for example, were indistinguishable from *mid H15* phenotypes while the row 1/8 bristle phenotype appeared to be both non-ventral and non-dorsal. This indicates clearly that *mid* must also be required to induce ventral fate. One exception to this was the AB which was rescued in *Mad mid H15* triple mutant clones. The unique response of the AB suggests that only one branch of the *mid H15* pathway is required in this cell. Thus, despite appearing to be a simple on/off switch for ventral fate in the leg, the way *mid* accomplishes this switching is not the same in all ventral cell lineages. In the AB, this may simply mean that the *mid* target genes required for AB development are all activated by Dpp and repressed by Mid. Consistent with this interpretation is the very weak rescue of AB by the repressor compromised mid^{eh1}. *mid H15* may also repress other default genes including genes that promote a default lateral fate or genes that promote a default dorsal fate that are regulated in parallel to Dpp. The repression of the laterally expressed reporter, *Upd*-lacZ, is consistent with such a role for *mid H15*.

mid H15 clearly act as repressors in ventral leg patterning, but can this explain their selector gene function? The mid^{eh1} mutant is almost completely compromised for *mid* gain-of-function effects. However, in rescue assays some *mid H15* mutant structures such as the row 1/8 bristles and the sex combs are substantially rescued. Thus mid^{eh1} clearly retains some *mid* function. Is this an activator function of *mid,* a residual repressor function, or perhaps both? There is clearly residual repressor function because mid^{eh1} is still able to partially repress the *VLE*-lacZ and *Upd*-lacZ target genes. Thus, the remaining rescuing activity in mid^{eh1} could reflect residual repressor activity. If it were possible to completely

and selectively remove the ability of *mid H15* to repress gene expression, it might lose all capacity to act as a ventral selector gene. There is also no formal reason to invoke that *mid H15* selector function also requires gene activation. Repression of default dorsal and lateral genes could explain *mid H15* function in dorsal ventral leg patterning. However, we do think it is very likely that *mid H15* has an activator role in the ventral leg because *mid H15* activates target genes in other fly tissues (Gaziova and Bhat, 2009; Reim et al., 2005) and we have only surveyed a small number of potential ventral target genes. In mouse, Tbx20 clearly acts as a repressor and an activator in both the developing and adult heart (Boogerd et al., 2018; Sakabe et al., 2012). Testing whether *mid H15* also encode activator functions in the leg will require further functional study of the T-box proteins to identify activator domains and the identification of more genes positively regulated by *mid H15*.

Acknowledgements

We thank Robert Holmgren, Krzysztof Jagla, Sandra Leal, Laurel Raftery, and Guy Tanentzapf for reagents. Stocks obtained from the Bloomington Drosophila Stock Center (NIH P40OD018537) were used in this study. L.A.P. was funded by a Queen Elizabeth Graduate Scholarship. This work was supported by the CIHR (Canada) (MOP-126035) and NSERC (Canada) (RGPIN/04828-2017).

Appendix A. Supplementary data

Supplementary data to this article can be found online at https://doi.org/10.1016/j.ydbio.2019.05.012.

References

Ayala-Camargo, A., Ekas, L.A., Flaherty, M.S., Baeg, G.H., Bach, E.A., 2007. The JAK/STAT pathway regulates proximo-distal patterning in Drosophila. Dev. Dynam. : Off. Publ. Am. Assoc. Anat. 236, 2721–2730.

Azpiazu, N., Morata, G., 2002. Distinct functions of homothorax in leg development in Drosophila. Mech. Dev. 119, 55–67.

Boogerd, C.J., Zhu, X., Aneas, I., Sakabe, N.J., Zhang, L., Sobreira, D.R., Montefiori, L.E., Bogomolovas, J., Joslin, A.C., Zhou, B., Chen, J., Nobrega, M., Evans, S.M., 2018. Tbx20 is required in mid-gestation cardiomyocytes and plays a central role in atrial development. Circ. Res. 123, 428–442.

Brook, W.J., 2010. T-box genes organize the dorsal ventral leg axis in Drosophila melanogaster. Fly (Austin) 4, 159–162.

Brook, W.J., Cohen, S.M., 1996. Antagonistic interactions between wingless and decapentaplegic responsible for dorsal-ventral pattern in the Drosophila Leg. Science 273, 1373–1377.

Brook, W.J., Ostafichuk, L.M., Piorecky, J., Wilkinson, M.D., Hodgetts, D.J., Russell, M.A., 1993. Gene expression during imaginal disc regeneration detected using enhancer-sensitive P-elements. Development 117, 1287–1297.

Buescher, M., Svendsen, P.C., Tio, M., Miskolczi-McCallum, C., Tear, G., Brook, W.J., Chia, W., 2004. Drosophila T box proteins break the symmetry of hedgehog-dependent activation of wingless. Curr. Biol. 14, 1694–1702.

Chen, H.B., Shen, J., Ip, Y.T., Xu, L., 2006. Identification of phosphatases for Smad in the BMP/DPP pathway. Genes Dev. 20, 648–653.

Chen, S., Kaneko, S., Ma, X., Chen, X., Ip, Y.T., Xu, L., Xie, T., 2010. Lissencephaly-1 controls germline stem cell self-renewal through modulating bone morphogenetic protein signaling and niche adhesion. Proc. Natl. Acad. Sci. U. S. A. 107, 19939–19944.

Curtiss, J., Halder, G., Mlodzik, M., 2002. Selector and signalling molecules cooperate in organ patterning. Nat. Cell Biol. 4, E48–E51.

Estella, C., Mann, R.S., 2008. Logic of Wg and Dpp induction of distal and medial fates in the Drosophila leg. Development 135, 627–636.

Estella, C., McKay, D.J., Mann, R.S., 2008. Molecular integration of wingless, decapentaplegic, and autoregulatory inputs into Distalless during Drosophila leg development. Dev. Cell 14, 86–96.

Estella, C., Voutev, R., Mann, R.S., 2012. A dynamic network of morphogens and transcription factors patterns the fly leg. Curr. Top. Dev. Biol. 98, 173–198.

Eusebio, N., Tavares, L., Pereira, P.S., 2018. CtBP represses Dpp-dependent Mad activation during Drosophila eye development. Dev. Biol. 442, 188–198.

Formaz-Preston, A., Ryu, J.R., Svendsen, P.C., Brook, W.J., 2012. The Tbx20 homolog Midline represses wingless in conjunction with Groucho during the maintenance of segment polarity. Dev. Biol. 369, 319–329.

Fulcoli, F.G., Huynh, T., Scambler, P.J., Baldini, A., 2009. Tbx1 regulates the BMP-Smad1 pathway in a transcription independent manner. PLoS One 4, e6049.

García-Bellido, A., 1975. Genetic control of wing disc development in *Drosophila*. In: Brenner, S. (Ed.), Cell Patterning, Ciba Found Symp. Associated Scientific Publishers, New York, pp. 161–182.

Gaziova, I., Bhat, K.M., 2009. Ancestry-independent fate specification and plasticity in the developmental timing of a typical Drosophila neuronal lineage. Development 136, 263–274.

Grimm, S., Pflugfelder, G.O., 1996. Control of the gene optomotor-blind in Drosophila wing development by decapentaplegic and wingless. Science 271, 1601–1604.

Hatashi, S., Ito, K., Sado, Y., Taniguchi, M., Akimoto, A., Takeuchi, H., Aigaki, T., Matsuzaki, F., Nakagoshi, H., Tanimura, T., Ueda, R., Uemura, T., Yoshihara, M., Goto, S., 2002. GETDB, a database compiling expression patterns and molecular locations of a collection of Gal4 enhancer traps. Genesis 34, 58–61.

Held, L.I., Heup, M.A., 1996. Genetic mosaic analysis of *decapentaplegic* and *wingless* gene function in the *Drosophila* leg. Dev. Gene. Evol. 206, 180–194.

Held, L.I., Heup, M.A., Sappington, J.M., Peters, S.D., 1994. Interactions of *decapentaplegic, wingless* and *Distal-less* in the *Drosophila* leg. Roux's Arch. Dev. Biol. 203, 310–319.

Heslip, T.R., Theisen, H., Walker, H., Marsh, J.L., 1997. Shaggy and dishevelled exert opposite effects on Wingless and Decapentaplegic expression and on positional identity in imaginal discs. Development 124, 1069–1078.

Ito, K., Awano, W., Suzuki, K., Hiromi, Y., Yamamoto, D., 1997. The Drosophila mushroom body is a quadruple structure of clonal units each of which contains a virtually identical set of neurones and glial cells. Development 124, 761–771.

Jagla, K., Frasch, M., Jagla, T., Dretzen, G., Bellard, F., Bellard, M., 1997. ladybird, a new component of the cardiogenic pathway in Drosophila required for diversification of heart precursors. Development 124, 3471–3479.

Jiang, J., Struhl, G., 1996. Complementary and mutually exclusive activities of decapentaplegic and wingless organize axial patterning during Drosophila leg development. Cell 86, 401–409.

Johnston, L.A., Schubiger, G., 1996. Ectopic expression of wingless in imaginal discs interferes with decapentaplegic expression and alters cell determination. Development 122, 3519–3529.

Leal, S.M., Qian, L., Lacin, H., Bodmer, R., Skeath, J.B., 2009. Neuromancer1 and Neuromancer2 regulate cell fate specification in the developing embryonic CNS of Drosophila melanogaster. Dev. Biol. 325, 138–150.

Lecuit, T., Brook, W.J., Ng, M., Calleja, M., Sun, H., Cohen, S.M., 1996. Two distinct mechanisms for long-range patterning by Decapentaplegic in the Drosophila wing. Nature 381, 387–393.

Lecuit, T., Cohen, S.M., 1997. Proximal-distal axis formation in the Drosophila leg. Nature 388, 139–145.

Lee, T., Luo, L., 1999. Mosaic analysis with a repressible cell marker for studies of gene function in neuronal morphogenesis. Neuron 22, 451–461.

Manjon, C., Sanchez-Herrero, E., Suzanne, M., 2007. Sharp boundaries of Dpp signalling trigger local cell death required for Drosophila leg morphogenesis. Nat. Cell Biol. 9, 57–63.

Mann, R.S., Carroll, S.B., 2002. Molecular mechanisms of selector gene function and evolution. Curr. Opin. Genet. Dev. 12, 592–600.

McCloy, R.A., Rogers, S., Caldon, C.E., Lorca, T., Castro, A., Burgess, A., 2014. Partial inhibition of Cdk1 in G(2) phase overrides the SAC and decouples mitotic events. Cell Cycle 13, 1400–1412.

Morimura, S., Maves, L., Chen, Y., Hoffmann, F.M., 1996. Decapentaplegic overexpression affects Drosophila wing and leg imaginal disc development and wingless expression. Dev. Biol. 177, 136–151.

Newfeld, S.J., Mehra, A., Singer, M.A., Wrana, J.L., Attisano, L., Gelbart, W.M., 1997. Mothers against dpp participates in a DDP/TGF-beta responsive serine- threonine kinase signal transduction cascade. Development 124, 3167–3176.

Pai, L.M., Orsulic, S., Bejsovec, A., Peifer, M., 1997. Negative regulation of armadillo, a wingless effector in Drosophila. Development 124, 2255–2266.

Pattatucci, A.M., Kaufman, T.C., 1991. The homeotic gene Sex combs reduced of Drosophila melanogaster is differentially regulated in the embryonic and imaginal stages of development. Genetics 129, 443–461.

Penton, A., Hoffmann, F.M., 1996. Decapentaplegic restricts the domain of wingless during Drosophila limb patterning. Nature 382, 162–164.

Reim, I., Mohler, J.P., Frasch, M., 2005. Tbx20-related genes, mid and H15, are required for tinman expression, proper patterning, and normal differentiation of cardioblasts in Drosophila. Mech. Dev. 122, 1056–1069.

Riese, J., Yu, X., Munnerlyn, A., Eresh, S., Hsu, S.C., Grosschedl, R., Bienz, M., 1997. LEF-1, a nuclear factor coordinating signaling inputs from wingless and decapentaplegic. Cell 88, 777–787.

Sakabe, N.J., Aneas, I., Shen, T., Shokri, L., Park, S.Y., Bulyk, M.L., Evans, S.M., Nobrega, M.A., 2012. Dual transcriptional activator and repressor roles of TBX20 regulate adult cardiac structure and function. Hum. Mol. Genet. 21, 2194–2204.

Singh, R., Horsthuis, T., Farin, H.F., Grieskamp, T., Norden, J., Petry, M., Wakker, V., Moorman, A.F., Christoffels, V.M., Kispert, A., 2009. Tbx20 interacts with smads to confine tbx2 expression to the atrioventricular canal. Circ. Res. 105, 442–452.

Staehling-Hampton, K., Jackson, P.D., Clark, M.J., Brand, M.H., Hoffmann, F.M., 1994. Specificity of bone morphogenetic protein-related factors: cell fate and gene expression changes in Drosophila embryos induced by decapentaplegic but not 60A. Cell Growth Differ. 5, 585–593.

Stennard, F.A., Costa, M.W., Lai, D., Biben, C., Furtado, M.B., Solloway, M.J., McCulley, D.J., Leimena, C., Preis, J.I., Dunwoodie, S.L., Elliott, D.E., Prall, O.W., Black, B.L., Fatkin, D., Harvey, R.P., 2005. Murine T-box transcription factor Tbx20 acts as a repressor during heart development, and is essential for adult heart integrity, function and adaptation. Development 132, 2451–2462.

Sun, Y.H., Tsai, C.J., Green, M.M., Chao, J.L., Yu, C.T., Jaw, T.J., Yeh, J.Y., Bolshakov, V.N., 1995. White as a reporter gene to detect transcriptional silencers specifying position-specific gene-expression during drosophila-melanogaster eye development. Genetics 141, 1075–1086.

Svendsen, P.C., Formaz-Preston, A., Leal, S.M., Brook, W.J., 2009. The Tbx20 homologs midline and H15 specify ventral fate in the Drosophila melanogaster leg. Development 136, 2689–2693.
Svendsen, P.C., Ryu, J.R., Brook, W.J., 2015. The expression of the T-box selector gene midline in the leg imaginal disc is controlled by both transcriptional regulation and cell lineage. Biol. Open 4, 1707–1714.
Takaesu, N.T., Hyman-Walsh, C., Ye, Y., Wisotzkey, R.G., Stinchfield, M.J., O'Connor, M.,B., Wotton, D., Newfeld, S.J., 2006. dSno facilitates baboon signaling in the Drosophila brain by switching the affinity of Medea away from Mad and toward dSmad2. Genetics 174, 1299–1313.
Theisen, H., Haerry, T.E., O'Connor, M.B., Marsh, J.L., 1996. Developmental territories created by mutual antagonism between Wingless and Decapentaplegic. Development 122, 3939–3948.
Tsuneizumi, K., Nakayama, T., Kamoshida, Y., Kornberg, T.B., Christian, J.L., Tabata, T., 1997. Daughters against dpp modulates dpp organizing activity in Drosophila wing development. Nature 389, 627–631.
Urrutia, H., Aleman, A., Eivers, E., 2016. Drosophila Dullard functions as a Mad phosphatase to terminate BMP signaling. Sci. Rep. 6, 32269.
Weiss, A., Charbonnier, E., Ellertsdottir, E., Tsirigos, A., Wolf, C., Schuh, R., Pyrowolakis, G., Affolter, M., 2010. A conserved activation element in BMP signaling during Drosophila development. Nat. Struct. Mol. Biol. 17, 69–76.
Wiersdorff, V., Lecuit, T., Cohen, S.M., Mlodzik, M., 1996. Mad acts downstream of Dpp receptors, revealing a differential requirement for dpp signaling in initiation and propagation of morphogenesis in the Drosophila eye. Development 122, 2153–2162.
Wodarz, A., 2008. Extraction and immunoblotting of proteins from embryos. Methods Mol. Biol. 420, 335–345.
Xu, T., Rubin, G.M., 1993. Analysis of genetic mosaics in developing and adult *Drosophila* tissues. Development 117, 1223–1237.
Zeng, Y.A., Rahnama, M., Wang, S., Sosu-Sedzorme, W., Verheyen, E.M., 2007. Drosophila Nemo antagonizes BMP signaling by phosphorylation of Mad and inhibition of its nuclear accumulation. Development 134, 2061–2071.
Zhang, Y., Ungar, A., Fresquez, C., Holmgren, R., 1994. Ectopic expression of either the Drosophila gooseberry-distal or proximal gene causes alterations of cell fate in the epidermis and central-nervous-system. Development 120, 1151–1161.